

# Toosendanin Inhibits Colorectal Cancer Cell Growth Through the Hedgehog Pathway by Targeting SHH

**Meng Zhang**

Hangzhou Medical College

**Zhongyi Tao**

Hangzhou Medical College

**Lijuan Gao**

Hangzhou Medical College

**Fengyang Chen**

Hangzhou Medical College

**Yiping Ye**

Hangzhou Medical College

**Shifang Xu**

Hangzhou Medical College

**Wenkang Huang**

Hangzhou Medical College

**Xiaoyu Li** (✉ [775423305@qq.com](mailto:775423305@qq.com))

Hangzhou Medical College <https://orcid.org/0000-0001-9973-7464>

---

## Research Article

**Keywords:** Toosendanin, colorectal cancer, HT29 cells, Hedgehog signalling pathway, SHH ligand

**Posted Date:** December 30th, 2021

**DOI:** <https://doi.org/10.21203/rs.3.rs-1175728/v1>

**License:**  This work is licensed under a Creative Commons Attribution 4.0 International License.

[Read Full License](#)

---

# Abstract

Colorectal cancer (CRC) is one of the most common gastrointestinal cancers worldwide. It is complex and often fatal and is associated with a high disease-related mortality. The Hedgehog (Hh) signalling pathway plays indispensable roles in CRC. Many studies have proven that Shh is overexpressed in cancer stem cells (CSCs) and shown that SHH overexpression is positively correlated with CRC tumorigenesis. The development of new drugs to kill CRC cells through the Hh pathway is urgently needed. Toosendanin (TSN), a natural triterpenoid saponin extracted from the bark or fruit of *Melia toosendan* Sieb. et Zucc., has been proven to inhibit various tumours. Here, we demonstrated that TSN inhibited the CRC cell growth through the Hh signalling pathway by targeting SHH. TSN has promising potential as an antitumour agent for CRC treatment.

## 1. Introduction

Colorectal cancer (CRC) is a heterogeneous tumour with a cell population ranging from pluripotent to differentiated cells. CRC is the second most common cancer in women and the third most common cancer in men. The cancer stem cell (CSC) model of cancer proposes that CSCs are key in the initiation of cancer. CSCs have been the research focus in a range of cancers, including CRC.[1–3] Cancer cells undergo transformation processes through alternative mechanisms that enable resistance to the deleterious effects of different treatments. The major signalling pathways involved in development, such as the Hedgehog (Hh), Wnt, and PI3K-AKT pathways, also play vital roles in tumorigenesis and resistance to various anticancer therapies.[4, 5]

The Hh signalling pathway plays a vital role in regulating the proliferation, apoptosis, angiogenesis, invasion and metastasis of different types of cells as well as in maintaining internal homeostasis in humans. Components of the Hh pathway include secreted Hh glycoprotein ligands, the 12-transmembrane protein receptor Patched (Ptch), the 7-transmembrane protein SMO, the nuclear transcription factors GLI 1–3, suppressor of fused homolog (SUFU), and a series of downstream Hh target genes, such as Gli1, Gli2, Ptch, Cyclin D, Cyclin E, FoxM1, and c-Myc.[6, 7] In the absence of Hh ligands, Ptch inhibits SMO activity; subsequently, GLI2 and GLI3 are phosphorylated by protein kinase A (PKA), glycogen synthase kinase 3 (GSK3) and casein kinase 1 (CK1); the N-terminal domains of GLI2 and GLI3 are cleaved; and the resulting truncated proteins, each of which includes transcription repressor domains, translocate into the nucleus to inhibit downstream gene transcription.[8, 9] Three Hh activation modes exist in cancer, based on the implicated mechanism: the type I pattern is characterized by autonomous and ligand-independent Hh signalling and is usually active in meningiomas and rhabdomyosarcomas; the type II pattern involves ligand-dependent oncogenic Hh signalling through autocrine/juxtacrine hormones and is active in the breast, lung and ovary; and the type III pattern involves ligand-dependent Hh signalling via paracrine or reverse paracrine signals and is active in prostate and pancreatic cancers. Reports have indicated that Shh ligands play an important role in both canonical and nonclassical Hh pathways, and that noncanonical Hh signalling is a positive regulator of Wnt signalling

in CSC-enriched cancers such as CRC.[6, 10] Therefore, Shh inhibitors are promising drugs for CRC treatment.

Toosendanin (TSN), a triterpenoid saponin extracted from the bark or fruit of *Melia toosendan* Sieb. et Zucc., a traditional Chinese medicine that was used as an agricultural insecticide in ancient China.[7, 8] Recently, accumulating evidence has shown that TSN plays an antitumour role in various cancers, including gastric cancer,[9] osteosarcoma,[11] pancreatic cancer,[12] hepatocellular carcinoma[13] and glioblastoma,[14] through the induction of apoptosis[15] via the Wnt/ $\beta$ -catenin, MEK/Erk or PI3K/AKT pathway. However, the effect of TSN on the Hh pathway has never been studied. Our research also preliminarily revealed that the target of TSN might be SHH and that TSN can inhibit CRC growth by inhibiting the Hh pathway.

## 2. Materials And Methods

### 2.1. Reagents and antibodies

TSN was isolated from the bark of *Melia toosendan* Sieb. et Zucc. and identified by NMR spectroscopy. The purity of TSN was determined to be more than 99% by HPLC. Vismodegib was purchased from MedChemExpress (USA), actinomycin D (ACD) was purchased from MedChemExpress (USA), the mouse anti-SHH antibody (E-1, sc-365112) and mouse anti-SMO antibody (E-5, sc-166685) were purchased from Santa Cruz (USA), and the rabbit anti-GLI1 antibody and mouse anti-GAPDH antibody were purchased from Beyotime (Beijing).

### 2.2. Cell lines and cell culture

The HT-29 and NIH3T3 cell lines were purchased from the American Type Culture Collection (ATCC, American Type Culture Collection). All cells were routinely cultured according to the manufacturer's instructions.

### 2.3. Dual-luciferase assays

Cells transfected with the respective luciferase plasmids and Renilla-TK construct were seeded into 48-well plates. After various treatments were performed as indicated, the luciferase activities were detected using a dual-luciferase assay kit according to the manufacturer's instructions (Promega) with a luminometer. The firefly luciferase values were

normalized to the Renilla luciferase values.

### 2.4. CCK-8 assay

We used a CCK-8 assay to determine the proliferation ability of HT-29 cells. HT-29 cells were cultured and seeded into each well of 96-well plates ( $8 \times 10^3$  cells in 100  $\mu$ l/well). After incubation for 24 h in a humidified 5% CO<sub>2</sub> incubator at 37°C, DMSO or the test compounds at different concentrations (100  $\mu$ l/well) were added to each well for 24 h. Cells in the wells were incubated with fresh RPMI 1640 medium

supplemented with 10 µl/well CCK-8 working solution for 2 h at 37°C in 5% CO<sub>2</sub>. Then, we measured the OD values at 450 nm using a microplate reader.

## ***2.5. Quantitative reverse transcription–polymerase chain reaction (qRT-PCR) analysis***

Total RNA was extracted from TSN-treated or untreated HT-29 cells using TRIzol reagent (Tiangen; Beijing, China) following the manufacturer's protocol. A FastKing cDNA First-Strand Synthesis Kit and SuperReal PreMix Color (SYBR Green) Kit were purchased from Tiangen (Beijing, China). The primers used in this experiment were synthesized by Shanghai Sango, and the sequences were as follows:

GAPDH-F 5'GAGTCAACGGATTTGGTCGT'3

GAPDH-R 5'GACAAGCTTCCCGTTCTCAG'3

PTCH1'-F 5'ACTTCAAGGGGTACGAGTATGT'3

PTCH1'-R 5'TGCGACACTCTGATGAACCAC'3

SMO-F 5'GAAGTGCCCTTGGTTCGGA'3

SMO-R 5'GCAGGGTAGCGATTGAGTT'3

GLI1-F 5'AGGGAGTGCAGCCAATACAG'3

GLI1-R 5'ATTGGCCGGAGTTGATGTAG'3

SHH-F 5'GCGAGATGTCTGCTGCTAGT'3

SHH-R 5'CCCTTCATACCTTCCGCTGG'3

## **2.6. Western blot analysis**

After treatment with different concentrations of TSN for 24 h, HT-29 cells were lysed with RIPA lysis buffer containing a protease inhibitor (100×) for 1 h on ice. Cell lysates were collected and were then centrifuged for 30 min at 13000 rpm. The protein concentrations in the lysates were quantified with a BCA kit (Beyotime), and proteins were then denatured at 100°C for 5 min in 5× SDS loading buffer. Equal amounts of proteins were loaded and separated by 8% SDS-PAGE. Proteins were transferred onto polyvinylidene fluoride membranes (Immobilon-P Transfer Membranes, USA), blocked with 5% skim milk at room temperature for 2 h and incubated at 4°C overnight with various primary antibodies. Finally, membranes were coincubated with horseradish peroxidase (HRP)-conjugated secondary antibodies at room temperature for 2 h and visualized with a chemiluminescence imaging system (Amersham ImageQuant 800). Protein expression levels were semiquantitatively analysed with Image J software (National Institutes of Health, USA).

## **2.7. Cellular thermal shift assay (CETSA)**

CETSA was performed to confirm the interaction between SHH and TSN in vitro by Western blot analysis. The CETSA technique is based on ligand-induced stabilization of target proteins. In brief, HT29 cells cultured to 90% confluence in 6-well plates were treated with medium containing DMSO or TSN (1  $\mu$ M) for 12 h. After treatment, cells were isolated with trypsin, collected by centrifugation (1000 rpm, 5 min), and resuspended in phosphate-buffered saline (PBS). The cell suspension was divided equally into 6 PCR tubes and heated in a temperature gradient from 40°C to 65°C over 3 min. Subsequently, cells were analysed by Western blotting.

## **2.8. BODIPY-cyclopamine (BC) competitive binding assays**

HEK293T cells were cultured and seeded into each well of 24-well plates ( $1 \times 10^5$  cells in 500  $\mu$ l/well). At 80-90% confluence, the cells were transfected with a Human Flag-6  $\times$  His-tagged Smo expression vector (1  $\mu$ g/well) using Lipofectamine® 3000 Reagent (Thermo Fisher Scientific, Inc.) according to the manufacturer's instructions. After 48 h, the cells were treated with 12.5 nM BC and various concentrations of the test compounds before incubation at 37°C for 2–4 h. The cells in each well were washed twice with PBS (0.2 ml/well), fixed with 4% paraformaldehyde for 15 min at room temperature, washed two more times with PBS, stained with 0.1  $\mu$ g/ml DAPI solution for 15 min (0.1 ml/well), and finally observed and imaged with an IX-73 microscope (Olympus, Japan). The data are expressed as the percentage of BC incorporation compared with that observed with BC alone by ImageJ software.[16–18]

## **2.9. Design of the Shh small interfering RNA (siRNA) and silencing of gene expression with siRNA**

The custom-designed Shh-specific siRNA was purchased from Shanghai Sango. The sequences for the Shh siRNA were as follows: sense-5'CGACAUCAUAUUUAAGGAYtt3' and antisense-5'AUCCUUAUUAUGAUGUCGgg3'. In addition, a negative control nontargeting scrambled siRNA was purchased from Shanghai Sango. All experiments were performed in triplicate. The transfection mixtures were prepared by mixing Lipofectamine-RNAiMAX and Opti-MEM1 with each shh siRNA separately at room temperature. The combined diluted siRNA duplexes and Lipofectamine-RNAiMAX were incubated for 5 min at room temperature. Finally, the above transfection mixtures were added to culture plates. Transfection was performed for 24 h at 37°C in a CO<sub>2</sub> incubator. Then, TSN was added to the cultured cells and incubated in 5% CO<sub>2</sub> for 24 h, and cells were then harvested for protein analysis.[19]

## **2.10. Animals and in vivo tumor xenograft studies.**

Female BALB/c/nu/nu nude mice weighing about 18g were obtained from Zhejiang province

Experimental Animal Center. All animal experiments were approved by the Animal Ethics and Research Committee of Zhejiang. HT29 cells ( $5 \times 10^6$ ) were injected subcutaneously into the right flank of mice (n=16). When the tumor volume reached around 50mm<sup>3</sup>, mice were randomly divided into 2 groups: control (mice receiving saline; n=6), TSN (1 mg/kg; n=6),

The saline and TSN were intraperitoneally given once daily for 20 days. When the treatment began, the mean tumor volumes were calculated every day with a caliper, using the formula

volume = (length x width<sup>2</sup>)/2. The mice were sacrificed 24 h after the final dose and tumors were resected aseptically for weight and volume calculation. Besides, the tumors were fixed and

subjected to immunohistochemical analysis.

### *2.11. Statistical analysis*

Data are presented as means ± SDs. Student's t-test or one-way ANOVA was used for statistical analysis to compare the different groups in this study. Differences with  $P \leq 0.05$  were considered statistically significant.

## **3. Results**

### **3.1. TSN inhibited the Hh pathway**

To investigate the effect of TSN on Hh signalling pathway activity, we first evaluated its activity by dual luciferase reporter assays using a reporter cell line, Shh-Light 2, which is an NIH 3T3 cell line containing a stably integrated Gli-luciferase reporter. After treatment with varying concentrations of TSN ranging from 0.156 to 10 nM, the firefly luciferase intensities, which correlated with the inhibitory activity of Hh, were initially measured (Fig. 1). Firefly luciferase intensities were then normalized to the corresponding intensities of Renilla luciferase, which was stably cotransfected into cells to evaluate the transfection efficiency and exclude false positive results caused by general cytotoxicity. The bioactivity results demonstrated that TSN displayed better inhibitory activity, with an  $IC_{50}$  value of 0.827 nM. Furthermore, this result demonstrated that the anticancer activity of TSN is closely related to the Hh pathway.

### **3.2. TSN inhibited CRC cell growth**

To explore the effects of TSN on HT-29 CRC cells, the antiproliferative activity of TSN was evaluated. The HT-29 cell line was incubated for 24 h after treatment with different concentrations of TSN, and CCK-8 assays were then carried out. Fig. 2 shows that the viability of TSN-treated cells decreased in a concentration-dependent manner and that the  $IC_{50}$  value of TSN in HT-29 cells was 0.346  $\mu$ M.

### **3.3. TSN regulated the mRNA levels of Hh signalling pathway components in HT-29 cells**

To explore the mechanism by which TSN inhibits the proliferation of HT-29 cells through the Hh signalling pathway, the mRNA levels of related Hh signalling pathway components were examined by qRT-PCR. In response to treatment with TSN for 24 h at concentrations ranging from 0.1  $\mu$ M to 3  $\mu$ M, the mRNA levels of SHH and SMO in the Hh signalling pathway were decreased in a dose-dependent manner. However, the

mRNA expression of GLI1 and PTCH was increased at low TSN concentrations. The GLI1 mRNA level was decreased only when the TSN concentration was 3  $\mu$ M, while no effect was observed for low TSN concentrations (Fig. 3). These results suggest that TSN might suppress HT-29 cell growth by inhibiting Hh signalling pathways. In addition, we speculated that TSN might affect SHH or SMO directly and regulate GLI1 and PTCH1, which are Hh target genes via the canonical Hh pathway.

### **3.4. TSN suppressed the expression of the corresponding proteins in the Hh signalling pathway**

Having demonstrated that TSN-induced inhibition of HT29 colon cancer cell growth is closely related to the Hh pathway via regulation of the mRNA levels of the key signalling components, we then performed Western blot analysis to investigate the expression levels of the corresponding proteins. TSN significantly inhibited the protein expression of SHH, SMO and GLI1 in a concentration-dependent manner (Fig. 4).

### **3.5. TSN inhibited Hh pathway signalling at the level of SHH**

Our previous experiments showed that the inhibitory effect of TSN on HT-29 cell growth was closely related to the Hh pathway, with significantly altered regulation of SHH expression. We thus speculated that TSN inhibits the canonical Hh pathway by downregulating SHH. To further explore the mechanism which TSN inhibits HT29 cell growth, we conducted CETSA, analysed mRNA half-lives after inhibition of transcription and performed an assay of competitive binding to SMO to verify the target of TSN.

#### **3.5.1. TSN-SHH binding was measured by CETSA**

CETSA, which is based on ligand-induced stabilization of target proteins, was carried out to confirm the interaction between SHH and TSN in vitro by Western blot analysis.[20, 21] The thermal stability of SHH in HT29 cells was tested in the temperature range of 40-65°C after exposure to TSN for 12 h. The control cells were treated with DMSO. SHH was still clearly detectable in cells exposed to TSN but not in control cells (Fig. 5A and B). Thus, the thermal stability of SHH in TSN-pretreated cells was higher than that in control cells. Collectively, these results showed the specific binding of TSN to SHH in HT29 cells.

#### **3.5.2. TSN reduces the stability of SHH mRNA**

We evaluated the effect of TSN on the stability of SHH mRNA in HT-29 colon cancer cells by indirectly analysing the mRNA half-life after inhibition of transcription with ACD. Treatment with TSN obviously decreased the SHH mRNA half-life (Fig. 6), suggesting that TSN decreases the SHH mRNA level in CRC cells by promoting its degradation.[22]

#### **3.5.3. Competitive binding ability of TSN to SMO**

To determine whether the inhibitory potency of TSN against the Hh pathway is due to its targeting of SMO, we used BC, a cyclopamine derivative with a fluorescent label, to analyse the direct interaction of TSN with SMO. First, HEK293T cells were transfected with the wild-type SMO expression vector. The binding ability of TSN to SMO was tested at concentrations of 1  $\mu$ M and 3  $\mu$ M, based on the effective concentration determined in the previous experiment and the concentrations that were proven to be noncytotoxic considering the results of the MTT assay in HEK 293 T cells. The fluorescence intensity associated with BC binding to SMO was used to evaluate the ability of TSN to act on SMO. HEK293T cells overexpressing SMO and BC were used as negative controls. Compared with the findings in the negative control and positive drug control (vismodegib) cells, the findings in the TSN-treated cells indicated that TSN could not competitively bind with SMO at either 1  $\mu$ M or 3  $\mu$ M (Fig. 7). These results suggest that TSN does not directly affect SMO.

### **3.6. TSN might not only regulate the canonical/SHH-SMO-GLI Hh pathway but also the non-canonical Hh pathway**

In the present study, we demonstrated that TSN inhibits HT29 cells at the level of the SHH ligand. To further determine the specific regulatory mechanisms of TSN, we first knocked down SHH in HT29 cells with siRNA targeting SHH (designated Shh-siRNA) before treatment with TSN at different concentrations and then analysed the relative expression of proteins in the canonical Hh pathway (Fig. 8) compared with that in control HT29 cells (Fig. 4). Western blot analysis showed that TSN also significantly inhibited the expression of SHH. Interestingly, SMO and GLI protein expression differed from GLI and SMO protein expression in the absence of SHH siRNA transfection. These relative expression levels, which were confirmed by Western blot analysis quantitative densitometric analysis, support the hypothesis that TSN might regulate not only the canonical SHH-SMO-GLI Hh pathway but also the non-canonical Hh pathway.

### **3.7. Effects of TSN administration on xenograft tumor growth.**

To further evaluate the in vivo antitumor effects of TSN, a nude mouse xenograft model was used for our animal study. HT29 cells were subcutaneously inoculated into nude mice. Mice were injected with vehicle, control (mice receiving saline; n=6, i.p.), TSN (1 mg/kg; n=6, i.p.)

for 20 days. As shown in Fig. 9, TSN significantly suppressed the tumor weight of the HT29 xenografts compared with control which demonstrating that TSN could effectively inhibit the growth of CRC cells in a xenograft model. At the same time, the tumor tissues were subjected to H&E staining and immunohistochemical analysis. The protein expression level of SHH in animal groups treated with TSN were significantly lower than those in other groups (Fig. 9). Thus, TSN strongly sensitizes colorectal cancer cells towards SHH expression in vivo.

## **4. Discussion**

Colon cancer is one of the most common malignancies worldwide. Its pathogenesis is complex and requires accumulated alterations in multiple genes and pathways.[23–26] Moreover, the interactions among these pathways are precise and complicated. These complexities also lead to the difficulties in drug treatment of CRC. Natural bioactive products may be key resources for new drug candidates. TSN, a naturally occurring triterpenoid saponin derived from the bark or fruit of *Melia toosendan* Sieb. et Zucc., was shown to have promising antitumour efficacy both in vitro and in vivo.

In our study, we first used a screening approach in SHH-light 2 cells to demonstrate that TSN can regulate the Hh pathway. Based on these findings, we speculated that the anticancer mechanisms of TSN are related to the Hh pathway, a previously unreported relationship. Our data obviously suggested that TSN can suppress the growth of HT29 CRC cells and revealed that TSN regulates the mRNA and protein levels of Hh signalling pathway components in HT-29 cells. Therefore, we determined that the inhibitory effect of TSN on CRC cell growth was closely related to the Hh pathway. Our data suggested that among the evaluate proteins, SHH showed the most obvious decreasing trend in expression under TSN treatment. We thus hypothesized that SHH may be a target of Hh pathway regulation and further carried out CETSA to prove our hypothesis. CETSA, a biophysical assay that allows the measurement of target engagement (TE) in intact cells and tissues, can directly assess drug binding at the target protein level (the protein reports) by applying the critical heating step while cells are still intact and the target protein is in its proper cellular environment. The CETSA results suggested that TSN can bind to SHH directly. Moreover, the BC competitive binding assay and the SHH mRNA stability assay also helped us to confirm that TSN inhibits CRC cell growth through the Hh pathway at the level of SHH.

Both the canonical and noncanonical Hh signalling pathways play indispensable roles in many CRCs. [27–30] The canonical Hh signalling pathway has been found to affect the expression of growth factors in tumour cells to promote tumour cell proliferation. However, the role of the canonical Hh signalling pathway in colon cancers has recently been controversial, and some views hold that the canonical Hh signalling pathway is not active in some colon cancers[31–33] Based on these theories, we carried out the next experiment to verify whether TSN acts only on the canonical Hh pathway.

Interestingly, we transfected SHH siRNA into HT29 cells and treated them with TSN at different concentrations. HT29 cells transfected with SHH siRNA and then treated with TSN showed different GLI and SMO protein levels than those without SHH siRNA transfection. With increasing TSN concentration, the decreasing trend in SHH protein expression became more obvious. However, GLI and SMO protein expression exhibited an increasing trend with an increase in the TSN concentration from 0.3  $\mu\text{M}$  to 3  $\mu\text{M}$ . These results demonstrated that TSN not only regulates the canonical/SHH-SMO-GLI Hh pathway but also may induce effects due to influences on SHH-dependent noncanonical Hh signalling or as a result of cross-talk with other pathways. Combined with the previous conclusions in our study, the regulation of GLI mRNA and protein shows different rules by TSN, which may also be related to this. According to previous reports, TSN not only regulates Hedgehog signaling pathway, but also regulates WNT/  $\beta$ -catenin pathway, PI3K/AKT pathway, and TGF-  $\beta$  pathway[34, 35]. Therefore, the regulation of TSN on Hh pathway may be the result of multiple pathways. These possibilities need further exploration. This study

provides a new idea for the treatment of colon cancer, which has multiple subtypes and complex mechanisms, and indicates that the multipathway inhibitor TSN is a promising drug.

## Declarations

### Ethics approval

All animals were kept in a pathogen-free environment and fed ad lib. The procedures for care and use of animals were approved by the Institutional Animal Care and use Committee (IACUC), ZJCLA (April 30th 2021/ZJCLA-IACUC-20030030).

### Consent to participate

Not applicable

### Consent for publication

Authors are responsible for the correctness of the statements in the manuscript. The authors affirm that the participants have consented to publish their data in the journal.

### Availability of data and materials

All authors ensure that all data and materials as well as software applications and custom code support their published claims and comply with field standards.

### Competing interests

The authors declare no competing interests.

### Funding

This research was supported by the Zhejiang Provincial Natural Science Foundation of China (Grant No. LGF20H300001) and the National Natural Science Foundation of China (Grant No. 81803404).

### Authors' contributions

**Meng Zhang:** Experiments, Investigation, Methodology, Software, Formal analysis, drafted the first version of the manuscript and revised; **Zhongyi Tao, Lijuan Gao, Wenkang Huang, Shifang Xu:** Investigation, Methodology; **Xiaoyu Li, Yiping Ye:** Experiments design. **Fengyang Chen:** Revised the manuscript. All authors read and approved the final manuscript.

### Disclosure of potential conflicts of interest

We declare there are no potential conflicts of interest.

### Research involving Human Participants and/or Animals

Research involving animals were approved by the Institutional Animal Care and use Committee (IACUC), ZJCLA (April 30th 2021/ZJCLA-IACUC-20030030).

## Informed consent

Not applicable

## References

1. Ricci-Vitiani L, Fabrizio E, Palio E, De Maria R (2009) Colon cancer stem cells. *J Mol Med (Berl)* 87:1097–1104. <https://doi.org/10.1007/s00109-009-0518-4>
2. Kreso A, Dick JE (2014) Evolution of the cancer stem cell model. *Cell Stem Cell* 14:275–291. <https://doi.org/10.1016/j.stem.2014.02.006>
3. Shimokawa M, Ohta Y, Nishikori S, Matano M, Takano A, Fujii M, Date S, Sugimoto S, Kanai T, Sato T (2017) Visualization and targeting of LGR5<sup>+</sup> human colon cancer stem cells. *Nature* 545:187–192. <https://doi.org/10.1038/nature22081>
4. Van den Brink GR, Bleuming SA, Hardwick JC, Schepman BL, Offerhaus GJ, Keller JJ, Nielsen C, Gaffield W, Van Deventer SJ, Roberts DJ, Peppelenbosch MP (2004) Indian Hedgehog is an antagonist of Wnt signaling in colonic epithelial cell differentiation. *Nat Genet* 36:277–282. <https://doi.org/10.1038/ng1304>
5. Chen H, Xu J, Hong J, Tang R, Zhang X, Fang JY (2014) Long noncoding RNA profiles identify five distinct molecular subtypes of colorectal cancer with clinical relevance. *Mol Oncol* 8:1393–1403. <https://doi.org/10.1016/j.molonc.2014.05.010>
6. Van Dop WA, Uhmman A, Wijgerde M, Sleddens-Linkels E, Heijmans J, Offerhaus GJ, Van den Bergh Weerman MA, Boeckxstaens GE, Hommes DW, Hardwick JC, Hahn H, Van den Brink GR (2009) Depletion of the colonic epithelial precursor cell compartment upon conditional activation of the hedgehog pathway. *Gastroenterology* 136:2195–2203.e2191–2197. <https://doi.org/10.1053/j.gastro.2009.02.068>
7. Fang XF, Cui ZJ (2011) The anti-botulism triterpenoid toosendanin elicits calcium increase and exocytosis in rat sensory neurons. *Cell Mol Neurobiol* 31:1151–1162. <https://doi.org/10.1007/s10571-011-9716-z>
8. He Y, Wang J, Liu X, Zhang L, Yi G, Li C, He X, Wang P, Jiang H (2010) Toosendanin inhibits hepatocellular carcinoma cells by inducing mitochondria-dependent apoptosis. *Planta Med* 76:1447–1453. <https://doi.org/10.1055/s-0029-1240902>
9. Zhou Q, Wu X, Wen C, Wang H, Wang H, Liu H, Peng J (2018) Toosendanin induces caspase-dependent apoptosis through the p38 MAPK pathway in human gastric cancer cells. *Biochem Biophys Res Commun* 505:261–266. <https://doi.org/10.1016/j.bbrc.2018.09.093>
10. Regan JL, Schumacher D, Staudte S et al (2017) Non-canonical Hedgehog signaling is a positive regulator of the WNT pathway and is required for the survival of colon cancer stem cells. *Cell Rep*

- 21:2813–2828. <https://doi.org/10.1016/j.celrep.2017.11.025>
11. Zhang T, Li J, Yin F, Lin B, Wang Z, Xu J, Wang H, Zuo D, Wang G, Hua Y, Cai Z (2017) Toosendanin demonstrates promising antitumor efficacy in osteosarcoma by targeting STAT3. *Oncogene* 36:6627–6639. <https://doi.org/10.1038/onc.2017.270>
  12. Pei Z, Fu W, Wang G (2017) A natural product toosendanin inhibits epithelial-mesenchymal transition and tumor growth in pancreatic cancer via deactivating Akt/mTOR signaling. *Biochem Biophys Res Commun* 493:455–460. <https://doi.org/10.1016/j.bbrc.2017.08.170>
  13. Liu XL, Wang H, Zhang L, Wang YL, Wang J, Wang P, He X, He YJ (2016) Anticancer effects of crude extract from *Melia toosendan* Sieb. et Zucc on hepatocellular carcinoma in vitro and in vivo. *Chin J Integr Med* 22:362–369. <https://doi.org/10.1007/s11655-015-2084-7>
  14. Cao L, Qu D, Wang H, Zhang S, Jia C, Shi Z, Wang Z, Zhang J, Ma J (2016) Toosendanin exerts an anti-cancer effect in glioblastoma by inducing estrogen receptor beta- and p53-mediated apoptosis. *Int J Mol Sci* 17:1928. <https://doi.org/10.3390/ijms17111928>
  15. Tang MZ, Wang ZF, Shi YL (2004) Involvement of cytochrome c release and caspase activation in toosendanin-induced PC12 cell apoptosis. *Toxicology* 201:31–38. <https://doi.org/10.1016/j.tox.2004.03.023>
  16. Infante P, Alfonsi R, Ingallina C et al (2016) Inhibition of Hedgehog-dependent tumors and cancer stem cells by a newly identified naturally occurring chemotype. *Cell Death Dis* 7:e2376. <https://doi.org/10.1038/cddis.2016.195>
  17. Zhu M, Wang H, Wang C, Fang Y, Zhu T, Zhao W, Dong X, Zhang X (2019) L-4, a Well-Tolerated and Orally Active Inhibitor of Hedgehog Pathway, Exhibited Potent Anti-tumor Effects Against Medulloblastoma in vitro and in vivo. *Front Pharmacol* 10:89. <https://doi.org/10.3389/fphar.2019.00089>
  18. Gao LJ, Zhang MZ, Li XY, Huang WK, Xu SF, Ye YP (2021) Steroidal alkaloids isolated from *Veratrum grandiflorum* Loes. as novel Smoothed inhibitors with anti-proliferation effects on DAOY medulloblastoma cells. *Bioorg Med Chem* 39:116166. <https://doi.org/10.1016/j.bmc.2021.116166>
  19. Islam SS, Mokhtari RB, Noman AS, Uddin M, Rahman MZ, Azadi MA, Zlotta A, Van der Kwast T, Yeger H, Farhat WA (2016) Sonic hedgehog (Shh) signaling promotes tumorigenicity and stemness via activation of epithelial-to-mesenchymal transition (EMT) in bladder cancer. *Mol Carcinog* 55:537–551. <https://doi.org/10.1002/mc.22300>
  20. Li Z, Zhang Y, Chen L, Li H (2018) The dietary compound luteolin inhibits pancreatic cancer growth by targeting BCL-2. *Food Funct* 9:3018–3027. <https://doi.org/10.1039/c8fo00033f>
  21. Langeback A, Bacanu S, Laursen H et al (2019) CETSA-based target engagement of taxanes as biomarkers for efficacy and resistance. *Sci Rep* 9:19384. <https://doi.org/10.1038/s41598-019-55526-8>
  22. Shen ZQ, Wang J, Tan WF, Huang TM (2021) Berberine inhibits colorectal tumor growth by suppressing SHH secretion. *Acta Pharmacol Sin* 42:1190–1194. <https://doi.org/10.1038/s41401-020-00514-2>

23. Williams CS, Bernard JK, Demory Beckler M, Almohazey D, Washington MK, Smith JJ, Frey MR (2015) ERBB4 is over-expressed in human colon cancer and enhances cellular transformation. *Carcinogenesis* 36:710–718. <https://doi.org/10.1093/carcin/bgv049>
24. Pernicova I, Korbonits M (2014) Metformin–mode of action and clinical implications for diabetes and cancer. *Nat Rev Endocrinol* 10:143–156. <https://doi.org/10.1038/nrendo.2013.256>
25. Alvarez-Medina R, Cayuso J, Okubo T, Takada S, Marti E (2008) Wnt canonical pathway restricts graded Shh/Gli patterning activity through the regulation of Gli3 expression. *Development* 135:237–247. <https://doi.org/10.1242/dev.012054>
26. Irshad S, Bansal M, Guarnieri P et al (2017) Bone morphogenetic protein and Notch signalling crosstalk in poor-prognosis, mesenchymal-subtype colorectal cancer. *J Pathol* 242:178–192. <https://doi.org/10.1002/path.4891>
27. Taipale J, Beachy PA (2001) The Hedgehog and Wnt signalling pathways in cancer. *Nature* 411:349–354. <https://doi.org/10.1038/35077219>
28. Konstantinou D, Bertaux-Skeirik N, Zavros Y (2016) Hedgehog signaling in the stomach. *Curr Opin Pharmacol* 31:76–82. <https://doi.org/10.1016/j.coph.2016.09.003>
29. Haveri H, Westerholm-Ormio M, Lindfors K, Maki M, Savilahti E, Andersson LC, Heikinheimo M (2008) Transcription factors GATA-4 and GATA-6 in normal and neoplastic human gastrointestinal mucosa. *BMC Gastroenterol* 8:9. <https://doi.org/10.1186/1471-230X-8-9>
30. Chung JH, Bunz F (2013) A loss-of-function mutation in PTCH1 suggests a role for autocrine hedgehog signaling in colorectal tumorigenesis. *Oncotarget* 4:2208–2211. <https://doi.org/10.18632/oncotarget.1651>
31. Guleng B, Tateishi K, Ohta M, Asaoka Y, Jazag A, Lin LJ, Tanaka Y, Tada M, Seto M, Kanai F, Kawabe T, Omata M (2006) Smoothed gene mutations found in digestive cancer have no aberrant Hedgehog signaling activity. *J Gastroenterol* 41:1238–1239. <https://doi.org/10.1007/s00535-006-1955-2>
32. Chatel G, Ganeff C, Boussif N, Delacroix L, Briquet A, Nolens G, Winkler R (2007) Hedgehog signaling pathway is inactive in colorectal cancer cell lines. *Int J Cancer* 121:2622–2627. <https://doi.org/10.1002/ijc.22998>
33. Alinger B, Kiesslich T, Datz C, Aberger F, Strasser F, Berr F, Dietze O, Kaserer K, Hauser-Kronberger C (2009) Hedgehog signaling is involved in differentiation of normal colonic tissue rather than in tumor proliferation. *Virchows Arch* 454:369–379. <https://doi.org/10.1007/s00428-009-0753-7>
34. Wang H, Wen C, Chen S et al (2020) Toosendanin-induced apoptosis in colorectal cancer cells is associated with the kappa-opioid receptor/beta-catenin signaling axis. *Biochem Pharmacol* 177:114014. <https://doi.org/10.1016/j.bcp.2020.114014>
35. Kai W, Yating S, Lin M, Kaiyong Y, Baojin H, Wu Y, Fangzhou Y, Yan C (2018) Natural product toosendanin reverses the resistance of human breast cancer cells to adriamycin as a novel PI3K inhibitor. *Biochem Pharmacol* 152:153-164. <https://doi.org/10.1016/j.bcp.2018.03.022>

## Figures

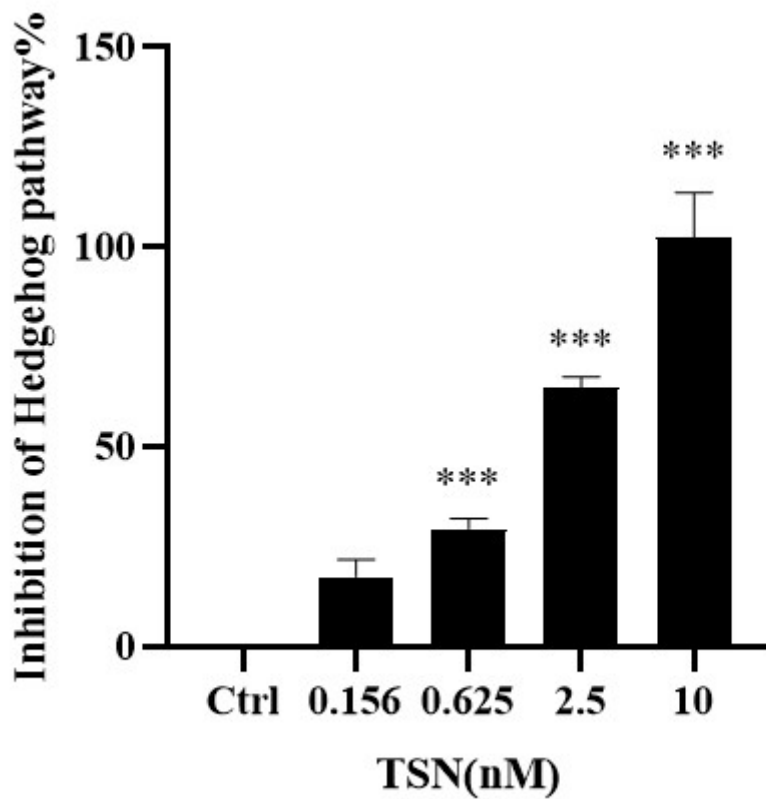
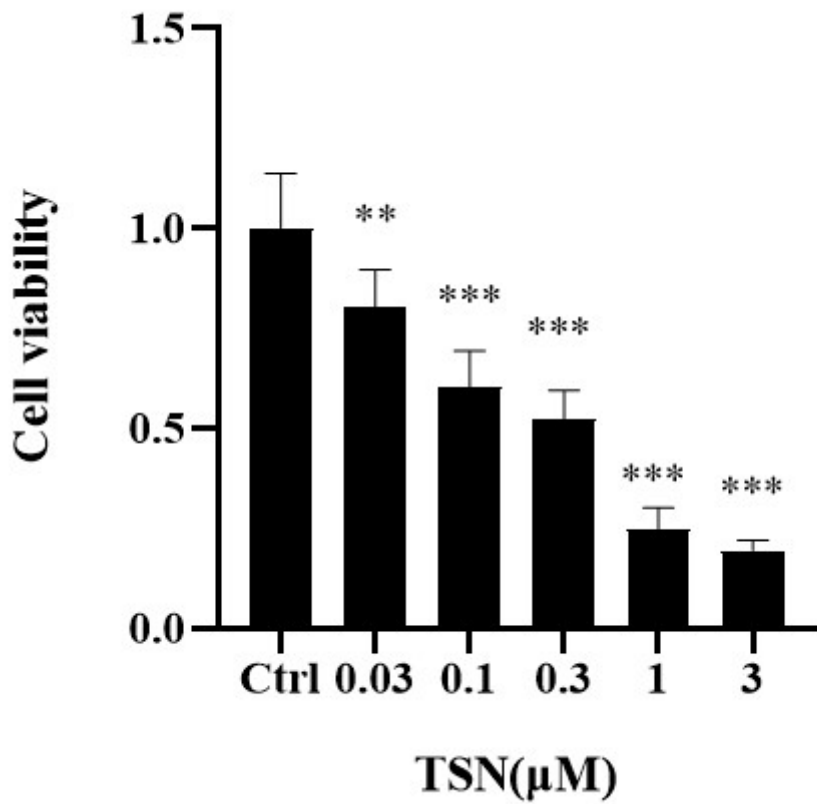


Figure 1

TSN inhibited the Hh pathway. TSN inhibited the Gli-responsive promoter in the Shh Light II cell line in a dose-dependent manner. Each experiment was performed with triplicates at least three times. One-way ANOVA was performed to calculate P values. \*P < 0.05, \*\*P < 0.01, and \*\*\*P < 0.001 compared to the control group. Ctrl, control



**Figure 2**

TSN inhibited the growth of HT-29 colon cancer cells in vitro. HT-29 cells were treated with the indicated concentrations of TSN for 24 h. Cell viability was evaluated using a CCK-8 assay, and the OD<sub>450 nm</sub> ratios of TSN-treated/untreated cells are indicated. The data are representative of six independent experiments. \*P< 0.05, \*\*P< 0.01, and \*\*\*P< 0.001 compared to the control group. Ctrl, control

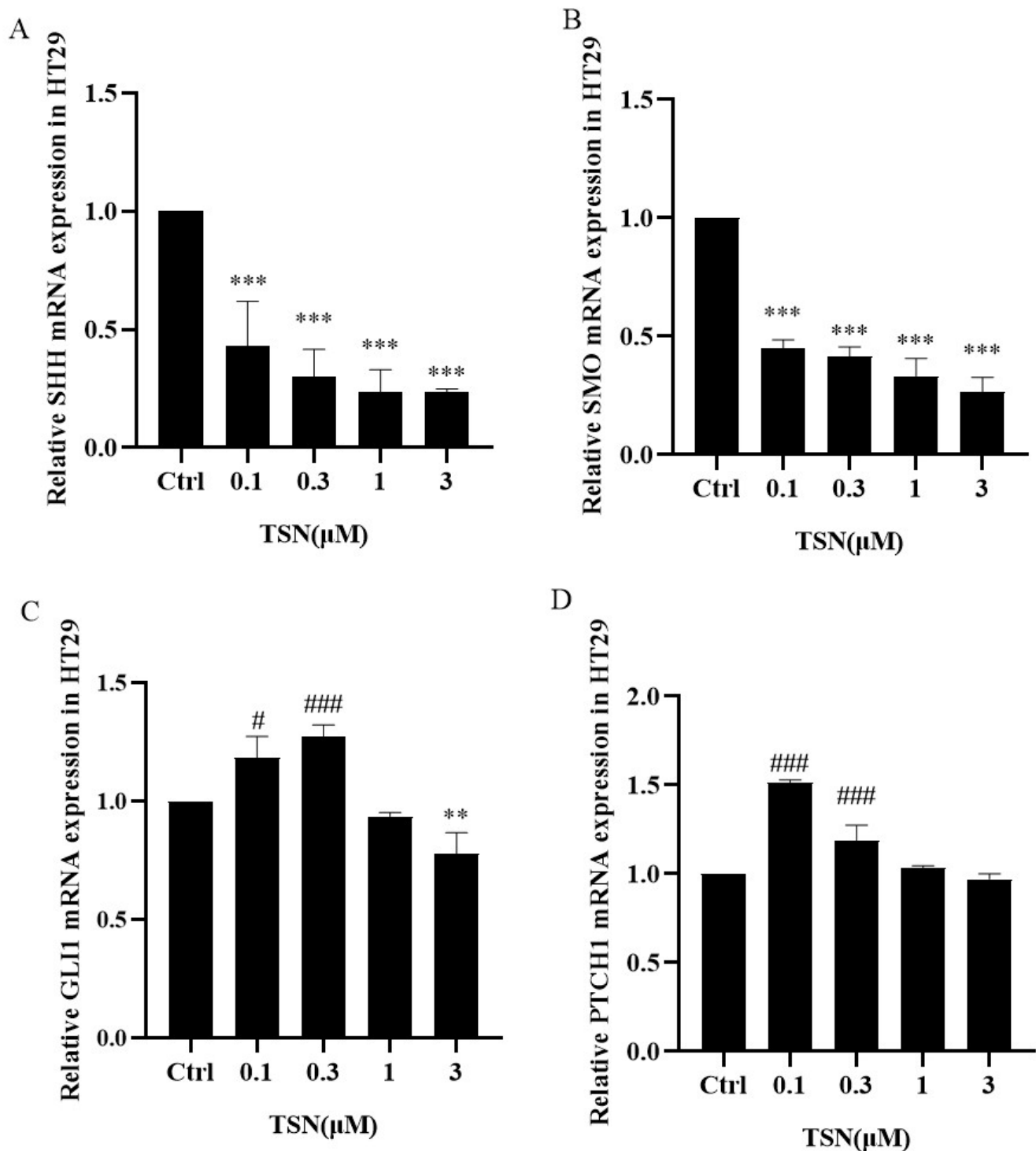


**Figure 3**

RT-qPCR analysis of mRNA expression of genes related to the Hh signalling pathway. HT-29 cells were stimulated with different concentrations of TSN (0.1, 0.3, 1 and 3 μM) for 24 h, and total mRNA was extracted. The mRNA levels of SHH, SMO, PTCH, SUFU, Gli1, and Gli2 were then measured by RT-qPCR. The data are expressed as the mean ± SD values; n= 3. #P< 0.05, ##P< 0.01, ###P<0.001, \*P< 0.05, \*\*P < 0.01, and \*\*\*P< 0.001 compared with the control group

**Figure 4**

HT-29 cells were stimulated with TSN for 24 h, and the protein expression levels of SHH, SMO and GLI1 were determined using Western blotting. Each treatment was performed in triplicate. The data are shown as the mean  $\pm$  SD values. \* $P < 0.05$ , \*\* $P < 0.01$ , and \*\*\* $P < 0.001$  compared with the control group.

**Figure 5**

TSN binding to SHH was confirmed by CETSA. CETSA was performed in HT29 cells treated with 1  $\mu$ M TSN or DMSO as the control. The stabilizing effect of TSN on the SHH protein was evaluated by Western blotting. Each treatment was performed in triplicate. The data are shown as the mean  $\pm$  SD values. \* $P < 0.05$ , \*\* $P < 0.01$ , and \*\*\* $P < 0.001$  compared with the control group.

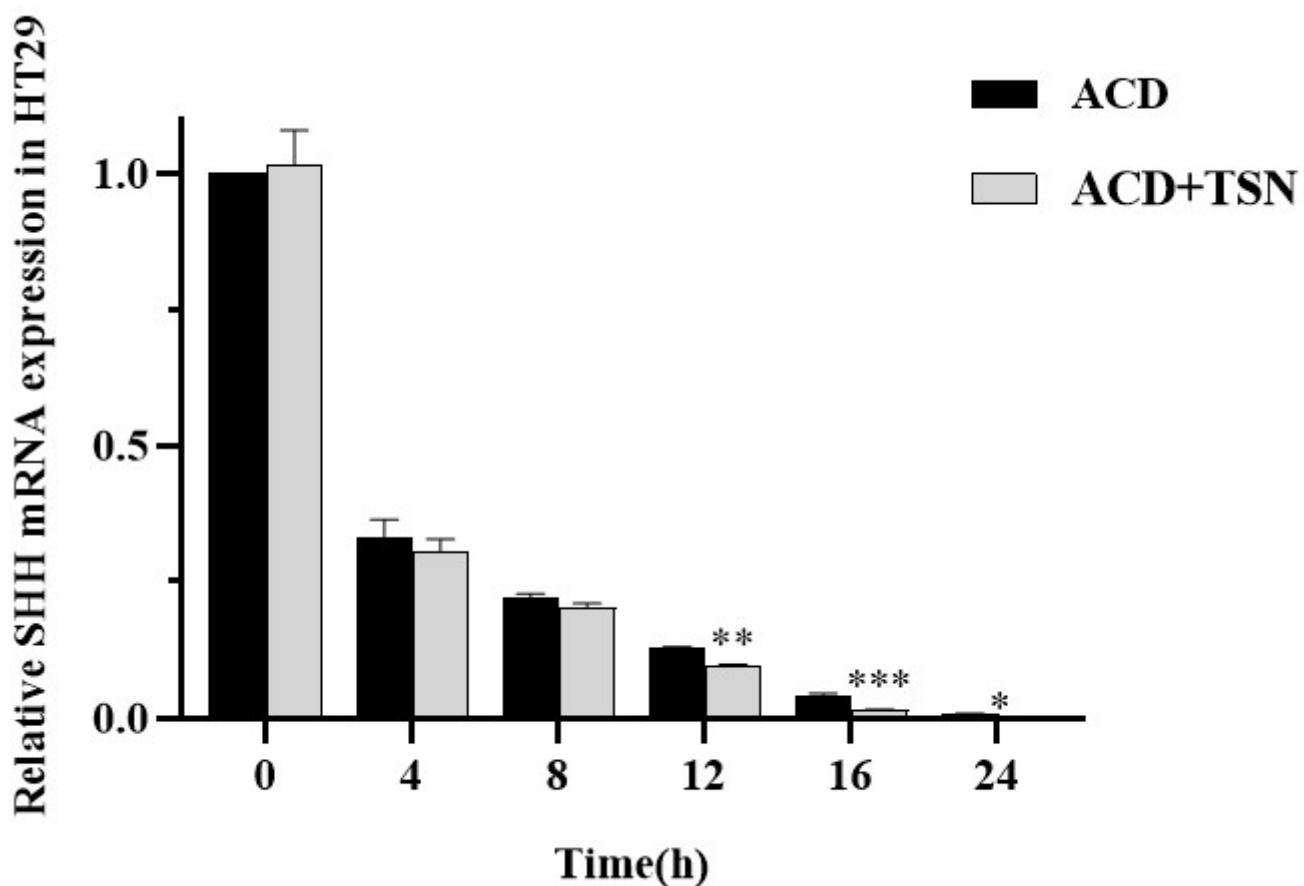


**Figure 6**

TSN reduces the stability of SHH mRNA. RT-qPCR analysis of SHH mRNA expression in HT-29 cells after treatment with ACD (10  $\mu$ M) with or without TSN (20  $\mu$ M) for the indicated times. The data are expressed

as the mean  $\pm$  SD values; n= 3. \*P < 0.05, \*\*P< 0.01, and \*\*\*P < 0.001 compared with ACD.

### SMO-overpression HEK293T cells

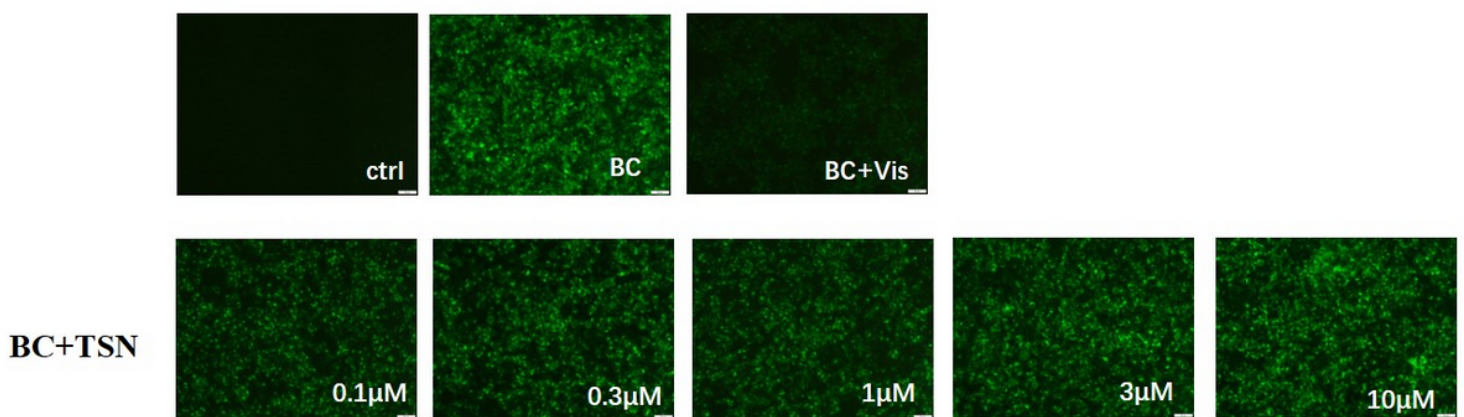


**Figure 7**

The TSN-induced ability of BC to bind to SMO in Smo-overexpressing HEK293T cells. Fluorescence images of TSN-induced BC binding to SMO in a concentration-dependent manner in HEK293T cells. Cells were exposed to 25 nM BC (green) and treated with DMSO or the test compounds (Vis, vismodegib) at different concentrations for 2–4 h, washed with chilled PBS, fixed with 4% paraformaldehyde for 15 min at room temperature, and washed two more times with PBS buffer for imaging by fluorescence microscopy (Ctrl: without BC).

**Figure 8**

Relative expression of Hh pathway proteins in HT29 cells transfected with SHH siRNA. (A) Western blot analysis of relative protein expression. Ctrl, transfected with empty vector; SHH siRNA+TSN, transfected with SHH siRNA and treated with different concentrations of TSN. (B, C, D) Western blotting was used to evaluate the expression levels of SHH, SMO, and GLI. Each treatment was performed in triplicate. The data were shown as the mean  $\pm$  SD values. \*P < 0.05, \*\*P < 0.01, and \*\*\*P < 0.001 compared with the SHH siRNA group; #P < 0.05 and ##P < 0.01 compared with the empty vector group

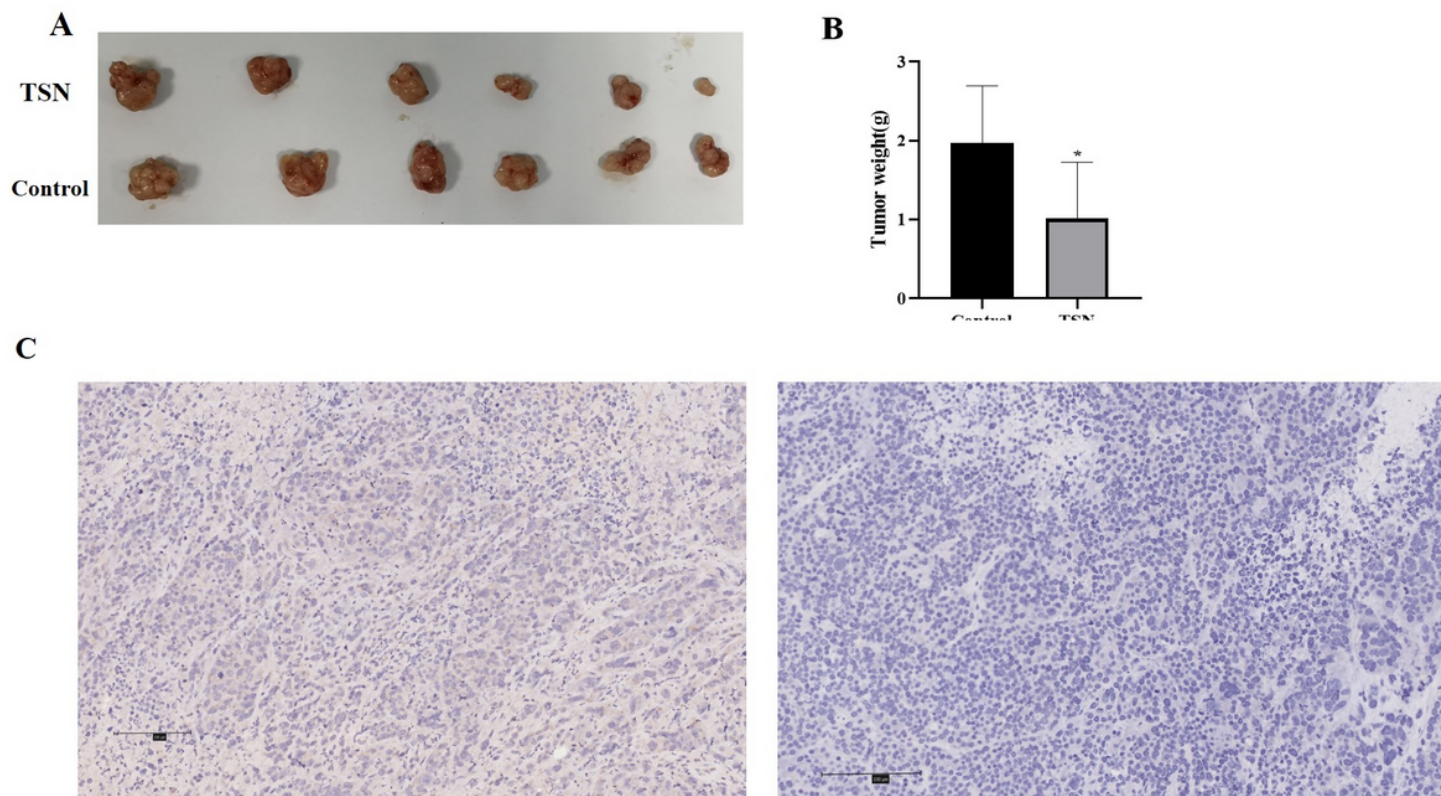


**Figure 9**

Inhibition of the growth of xenograft tumors derived from HT29 cells by TSN administration. **(A)** The image shows the difference of tumor volume between the TSN-treated groups and the control group on Day 20. **(B)** The differences of tumor weight between the TSN-treated groups and the control group were statistically significant ( $*P < 0.05$ ). **(C)** After treatment, the tumors were removed and subjected to H&E staining

analysis.

## Supplementary Files

This is a list of supplementary files associated with this preprint. Click to download.

- [SupplementtoFigure4threeindependentexperiments.jpg](#)
- [supplementtoFigure5threeindependentexperiments.jpg](#)
- [supplementtoFigure8threeindependentexperiments.jpg](#)